ORIGINAL ARTICLE

Utilization of streamflow rates for determination of precipitation thresholds for landslides in a data-scarce region (Eastern Bartın, NW Türkiye)

Pınar Avcı[1] · **Murat Ercanoglu**[1]

Abstract
One of the Türkiye's most destructive natural hazards is landslides. Although much progress has been achieved in this subject throughout the country, there are still some problems related to adequate meteorological and high-quality landslide data. The aim of this study, which was carried out in the eastern part of Bartın province in the Western Black Sea region of Türkiye, is to indirectly determine the possible threshold values for landslides known to be triggered by precipitation. For this purpose, first, data related to landslides, precipitation, and streamflow were compiled and analyzed. Although many landslides have been mapped in the area, it has been determined that the number of reliable data on the dates (only three exact dates) of landslide occurrences is quite limited in the area. The relationship between the landslides that occurred in 1985, 1998, and 2021, and the stream gauging–precipitation data was analyzed. Then, due to the data scarcity related to the precipitation data, an indirect method, called Soil Conservation Service Curve Number (SCS-CN), was used to determine the relation between runoff and precipitation. The results revealed that daily 80 mm and cumulative 160 mm could be selected as the threshold values that may trigger the landslides. This study serves as an illustration of how an indirect approach can be used to approximate potential precipitation thresholds in a data-scarce region. Therefore, it will be possible to use these precipitation thresholds as a basis for future landslide hazard and risk assessments.

Keywords Drainage density · Landslide · SCS-CN method · Streamflow

Introduction

What Brabb (1991) stated 32 years ago as if he guessed today: *"Landsliding is a worldwide problem that probably results in thousands of deaths and tens of billions of dollars of damage each year. Much of this loss would be avoidable if the problems were recognized early, and landsliding is likely to become more important to decision makers in the future"*. Considering Brabb's (1991) foresight and comments, it is obvious that these evaluations precisely reflect the actual conditions all around the world in terms of landslides. Accordingly, throughout the world, landslides still pose a threat to lives and cause damage to property as well as the environment. Türkiye, one of the landslide-suffering countries, has been valued nearly 10 times greater than the average value given for the world by CRED (2020) concerning landslide-related economic losses (Keles and Nefeslioglu 2021). The other significant statistics given by AFAD (Disaster and Emergency Management Presidency of Türkiye) have revealed that landslides are responsible for approximately 30% of the number of affected people by natural hazards in Türkiye in the last 70-year period (http://www.afad.gov.tr) (AFAD 2022). In Türkiye, particularly in the last two decades, many projects and mitigation efforts have been initiated by governmental agencies and local authorities to combat natural hazards. A governmental institution, namely AFAD, was established in 2009 for coordination and management of the disasters in the country, in cases of disaster and emergencies. AFAD initiated a new disaster management model for all natural hazards by considering susceptibility, hazard and risk assessments in overall Türkiye, identical to the developed countries. In this regard,

✉ Pınar Avcı
pavci@hacettepe.edu.tr

Murat Ercanoglu
murate@hacettepe.edu.tr

1 Geological Engineering Department, Hacettepe University, 06800 Beytepe/Ankara, Türkiye

the landslide inventory map of Türkiye has been updated on larger scales by AFAD's provincial branches throughout Türkiye, and this attempt has still been continuing to complete the landslide inventory of the whole territory in detail. These positive changes in disaster policies and measures of the country will minimize the possible losses and damages that may occur due to landslides in the near future.

When the landslide literature is analyzed, among the triggering factors of the landslides, precipitation is revealed as the most commonly considered factor by the researchers (e. g., Guzzetti et al. 2008; Lateh et al. 2013; Mandal and Maiti 2013; Wu and Chen 2013; Zhuang et al. 2014; Melillo et al. 2016; von Ruette et al. 2016; Li et al. 2017; Ghosh et al. 2019; Zhao et al. 2019; Leonarduzzi and Molnar 2020; Avila et al. 2021; Kim et al. 2021; Kim et al. 2022), in addition to earthquakes (e. g., Jibson and Harp 2016; Fan et al. 2018; Wang et al. 2018; Lombardo et al. 2019; Du and Pan 2020; Tanyas and Lombardo 2020). Whether triggered by rainfall, earthquake, or both (Sassa et al. 2007; Zhang et al. 2014), it is essential to evaluate the relation between triggering factors and landslides. This relation could be analyzed by deterministic and probabilistic models. Deterministic models in 2D and/or 3D describe the physical and/or mechanical behavior of slopes by considering various conditions and scenarios such as groundwater changes, ground acceleration, external loads, etc. (Firincioglu and Ercanoglu 2021). On the other hand, probabilistic models are based on the identification of rainfall and/or seismic thresholds that trigger the landslides. For example, if precipitation is considered as a landslide-triggering factor, it can be defined physically or empirically. Different types of empirical rainfall thresholds for the possible initiation of landslides have been proposed in the literature as the extent of the geographical area for which they were defined and the type of rainfall measurement used to establish the thresholds (Guzzetti et al. 2008). Of these, rainfall intensity–duration (I–D) thresholds (short-time landslide simulation) or cumulative rainfall (long-time landslide simulation) during a given period can be used to simulate the triggering factor of the landslide (Li et al. 2017). In this regard, historical records of landslides are of great importance. However, it is often not possible to reach such records in many regions, as in the case of this study. In addition, data scarcity and/or insufficiency related to the triggering factor of landslides is the other problematic issue in such a study.

Based on the reports, archive studies, and interviews with the local people in the study area, it was determined that the landslides in the region were exactly triggered by precipitation and no data exist related to any seismically induced landslide. Thus, in the first stage, we have stressed the landslides and rainfall data. Although there are hundreds of landslides in the area of concern and the landslide-triggering factor is reported as the rainfall, the exact time and

rainfall data are missing for many landslides in the area. Furthermore, there is only one meteorological station which does not reflect the precipitation regime itself because of the geographical features of the region including two different types of precipitation regime (terrestrial and frontal) within the boundary of the study area. Moreover, when the data of meteorological stations close to the study area are examined, it is revealed that they contain significant deficiencies concerning precipitation data.

Many scientists have attempted to analyze the relationship between precipitation and landslide occurrences to find the critical thresholds which can be categorized as physical (process based, conceptual) or empirical (historical, statistical) bases (Guzzetti et al. 2007). In addition, Zhuang et al. (2014) stated that the most common approaches to determine such thresholds are antecedent rainfall, antecedent effective rainfall, precipitation duration, precipitation intensity, cumulative rainfall, maximum hourly rainfall intensity, normalized rainfall, and daily rainfall. Of these, process-based thresholds may be useful particularly for landslide warning systems because they can predict the conditions such as the amount of precipitation, failure mechanism, and location to initiate a landslide (e. g., Fowze et al. 2012; Avila et al. 2021; Das et al. 2022). However, as can be seen from the landslide literature, the fact that it is based on many detailed and representative spatial data hinders the application of this method in large areas. Instead, it is preferred to be applied in individual landslides or small areas. In contrast, empirical thresholds are defined by studying rainfall events that have resulted in landslides and can be implemented on a regional, local or even global scale (Guzzetti et al. 2007). As Glade et al. (2000) stated it could be possible to establish a relationship between precipitation and landslides if sufficient and reliable data exist. Of course, to obtain statistically meaningful analysis for temporal and spatial landslide initiation based on precipitation thresholds, there must be sufficient stations and reliable data representing the area in concern. Indeed, reasonably reliable prediction of landsliding occurrence based on climatic thresholds has been accomplished in different parts of the world, where abundant weather stations are located at different elevations, and where sufficient data were available (Jakob and Weatherly 2003). In the literature, many excellent studies related to the determination of empirical precipitation thresholds and landslides have been performed (e.g., Brunetti et al. 2010; Tien Bui et al. 2013; Bhandary et al. 2013; Bai et al. 2014; Althuwaynee et al. 2015; Ramos-Canon et al. 2016; Hong et al. 2018; Marra 2019). However, it should be kept in mind that investigating the relationship between landslides and precipitation is a challenging task. Thus, the researchers have to work with the available data, even though they have deficiencies or limitations. Criteria for the objective and reproducible reconstruction of rainfall conditions that triggered landslides

are still lacking, poorly formalized, or ambiguous (Melillo et al. 2016). Under these conditions mentioned above, as emphasized by Jakob and Waetherly (2003), it is also possible to approach by investigating the relationship between precipitation and streamflow data. Therefore, in this study, it was preferred to approach with streamflow data that can be associated with the precipitation, which is more representative throughout the area.

Given the conditions above, streamflow data were preferred to analyze the triggering threshold, and then linked to the precipitation as an alternative approach by using Soil Conservation Service Curve Number (SCS-CN) (1985) method, detailed in USDA (1986). Since the inability to determine the spatial distribution of precipitation data prevented the determination of triggering threshold value of the landslides in the study area, it is aimed at analyzing streamflow data, which is considerably related to the precipitation. The spatial distribution of the flow on the tributary has been analyzed using streamflow rate data measured at 4 different stream gauging stations (SGS). Toward this end, by defining the precipitation–flowrate relationship, an approach has been made to determine the possible precipitation threshold values that can trigger landslides in the study area.

Study area

The study area is located in the Western Black Sea region of Türkiye. It covers an area of 1417.5 km^2 extending southeastward from 5 km east of Bartın city center (Fig. 1a) representing semi-mountainous region characteristics. The main settlements are Ulus, located in the central part of the study area, Abdipaşa and Kumluca districts. There are also many scattered villages throughout the study area and rural life is dominant in the region. This area is known as one of the most landslide-prone areas in Türkiye. For example, in 1985 and 1998, the Western Black Sea region, also including the study area, was declared as a regional disaster area by the decision of the Council of Ministers of Türkiye. In addition, there have been some landslide susceptibility and risk-related studies previously carried out in different parts of the study area (e. g., Ercanoglu 2005; Ercanoglu et al. 2008; Erener and Düzgün 2012, 2013). In the study area, a total of 1169 landslide locations (Fig. 1a and b) were compiled by the database gathered from governmental institutions in addition to field works carried out for this study. The areal extent of the average landslide size is 165,060 m^2. Minimum and maximum landslide sizes are 6245 m^2 and 2.95 km^2, respectively. Landslides are dominantly rotational earth slides in addition to complex type failures based on Varnes's (1978) classification.

Digital elevation model (DEM) of the study area was obtained from the General Directorate of Mapping of Türkiye with 20 m resolution (Fig. 2a). Topographical elevation ranges from 5 to 1735 m (a. s. l.) and close areas to the southern boundary cover the higher elevations in the region. Minimum and maximum slope values are 0° and 77°, respectively (Fig. 2b). Gentle slopes (below 10°) are abundantly located in the close vicinity of Bartın River and NW part of the study area, while steep slopes are generally in the eastern and northern sections. Approximately, 71% of the area varies between 10 and 30 degrees, while slopes higher than 40 degrees correspond to only 1.5% of the area. Ulus, Kocanoz, and Bartın rivers are the main rivers, and their tributaries form a dendritic drainage system (Fig. 2c) in the study area. Streams in the region fragmented the terrain, and thus, it represents a rough appearance. There are narrow and deep valleys in the study area, while flat plains, where the streams are widened, also exist. Concerning land use characteristics (Fig. 2d) given by Coordination of Information on the Environment (CORINE) (http://land.copernicus.eu) (CORINE 2006) for the year of 2006, 55.6% of the study area is covered by broad-leaved (33.1%) and mixed forest (22.5%), while the agricultural areas constitute the third most abundant land use group (16.9%) in the area. Agricultural lands and forests (mixed and broad-leaved), on the other hand, cover 31.2% and 25.1% of the landslide locations, respectively.

Geologically, the study area, located in the Western Pontides tectonic unit, consists of 15 different lithologies from Silurian–Devonian to Quaternary age (Fig. 2e). Particularly, in the eastern and the southern parts of the study area, sedimentary units with different ages have severely been deformed by folds and faults and represent complex geological characteristics (Yergök et al. 1987). The oldest lithology in the study area is Silurian–Devonian age limestones (Kub3). The Permo-Triassic terrestrial Çakraz formation (PTRc) and the Triassic Çakrazboz formation (Jh) are transitive with each other and overlie the older units with an angular unconformity. Upper Jurassic İnaltı Formation (JKi) is represented by limestone, which forms steepest topography in the region in addition to Lower Cretaceous limestones (Kus) and conglomerates (Kua). Lower Cretaceous–Cenomanian age Kilimli Formation (Kk) consists of sandstone–mudstone in addition to shales and marn alternations. Ulus Formation (Ku) is the most landslide-prone lithology in the study area and represents flysch characteristics, consisting of turbiditic sandstone, mudstone, and shale alternations. It is of Upper Cretaceous age and highly susceptible to weathering as well. Yemişliçay Formation (Ky) mainly contains volcano-sedimentary rocks in addition to shale and sandstone (Kyk). Maastrichtian–Lower Eocene age Akveren formation (KTa) is comprised of limestones with clay and is overlaid by Lower Eocene age andesite, dacite, and agglomerates of Yığılca formation (Tkisd). Lower–Middle Miocene age Çaycuma formation (Tc) consists of alternations of volcanic intercalated sandstone, siltstone, claystone, and shale.
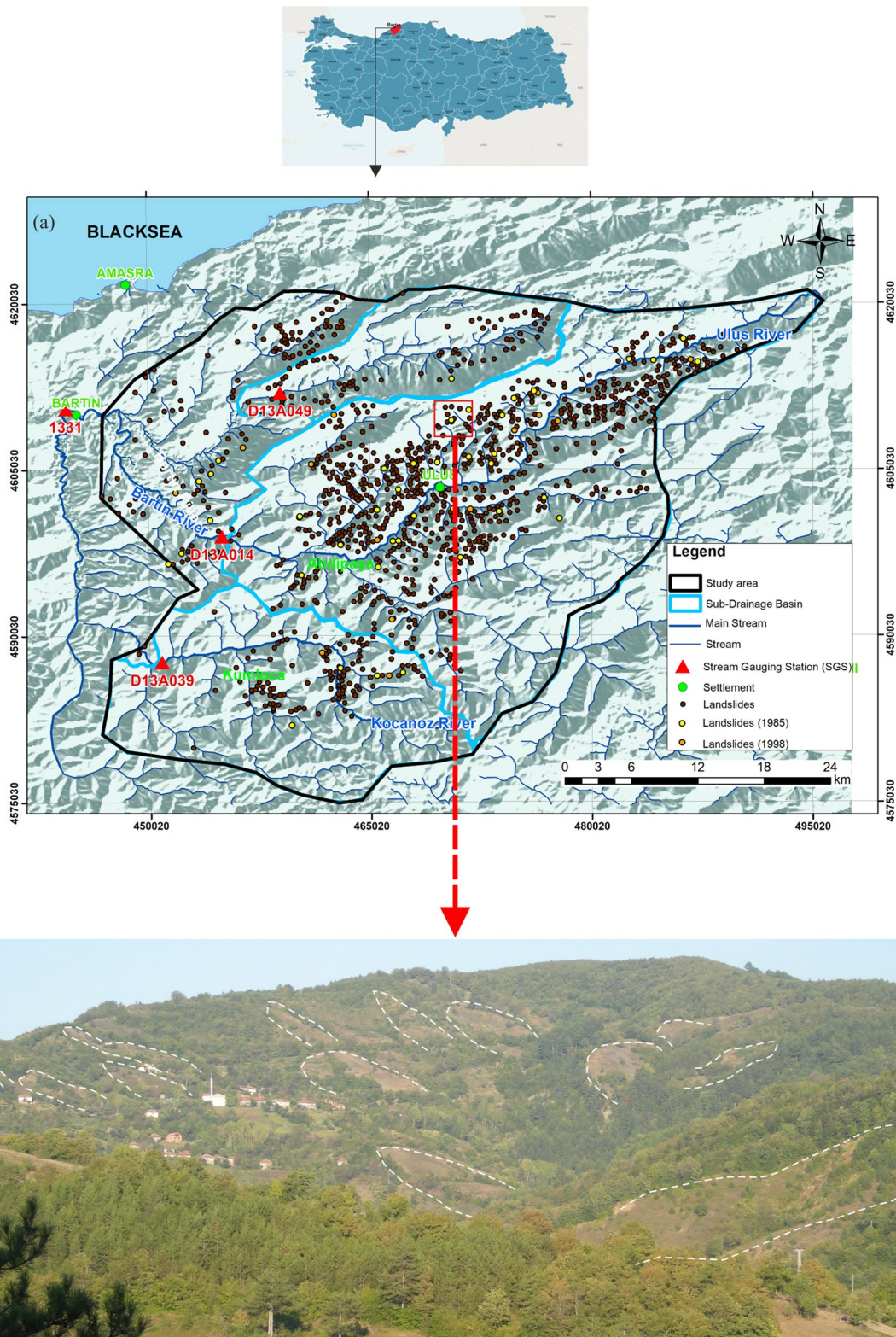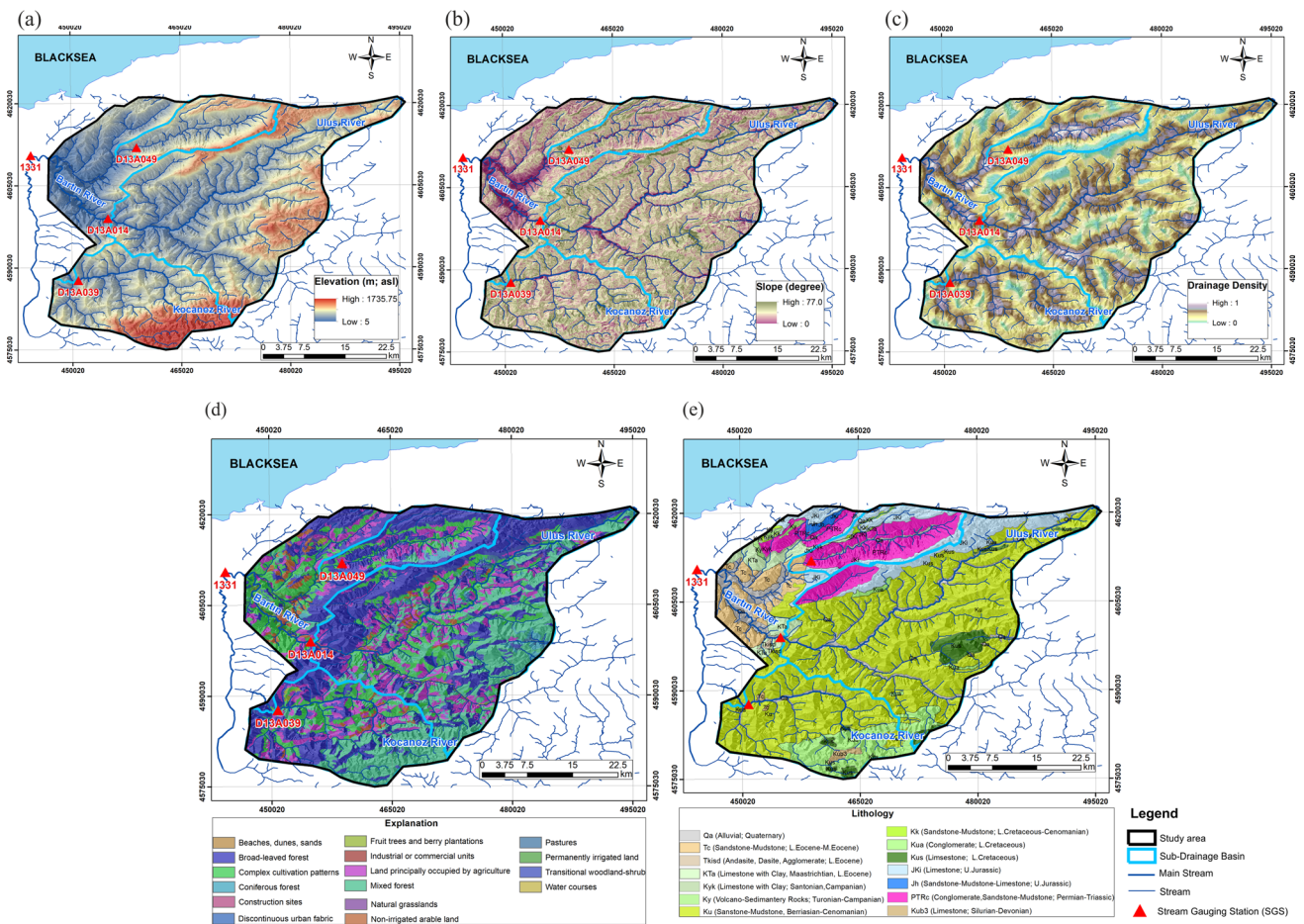
Fig. 1 Location map of the study area

Fig. 2 General characteristics of the study area **a** elevation; **b** slope; **c** drainage density; **d** land use and **e** lithology

Quaternary alluvial deposits unconformably overlies the older units. With respect to landslide occurrences, three lithologies, namely PTRc, KTa, and Ku (see Fig. 2e), mostly overlap (ca. 98%) with the landslide locations. Of these, Ku (Ulus Formation) includes 82% of the landslide locations. PTRc (Çakraz Formation) and KTa (Akveren Formation) are the second and third dominant lithologies where the landslide locations are included as 12% and 4%, respectively. The ratio of all remaining lithologies to include landslides is only 2%. It was revealed that the landslides occurred in the weathering zones of these lithologies. Based on the field observations, thickness of the weathering zones of these units starts from 1–2 m and reaches up to 40 m.

Methodology

This study mainly consists of three stages (Fig. 3) such as data collection and analysis, assessment of the spatial distribution of streamflow, and determination of possible precipitation thresholds by SCS-CN method. In the first stage,

data related to landslides, precipitation, drainage density, and streamflow were compiled, and their relationship was investigated.

Although more than 1000 landslide locations (see Fig. 1a) exist, only 81 of them have precisely been dated in the database. The research carried out in AFAD archives reveals two significant dates such as February 12, 1985, and May 21, 1998, in the study area. Based on the archive studies, although the number of deaths, injuries, and the total cost could not be determined, 1165 houses became unusable and many structures such as roads, mosques, and fountains were damaged because of these landslides. It is very likely that more than the mentioned 81 landslides have occurred and/ or re-activated in the study area. However, landslides, which were in official archive records and the ones close to the settlements, had to be considered for the current study.

Since the landslides were triggered by the precipitation, meteorological stations (MS) within and/or in the close vicinity of the study area were investigated by Turkish State Meteorological Service (MGM) archives (MGM 2022) (Fig. 4a). Based on the research, Ulus MS was the only one
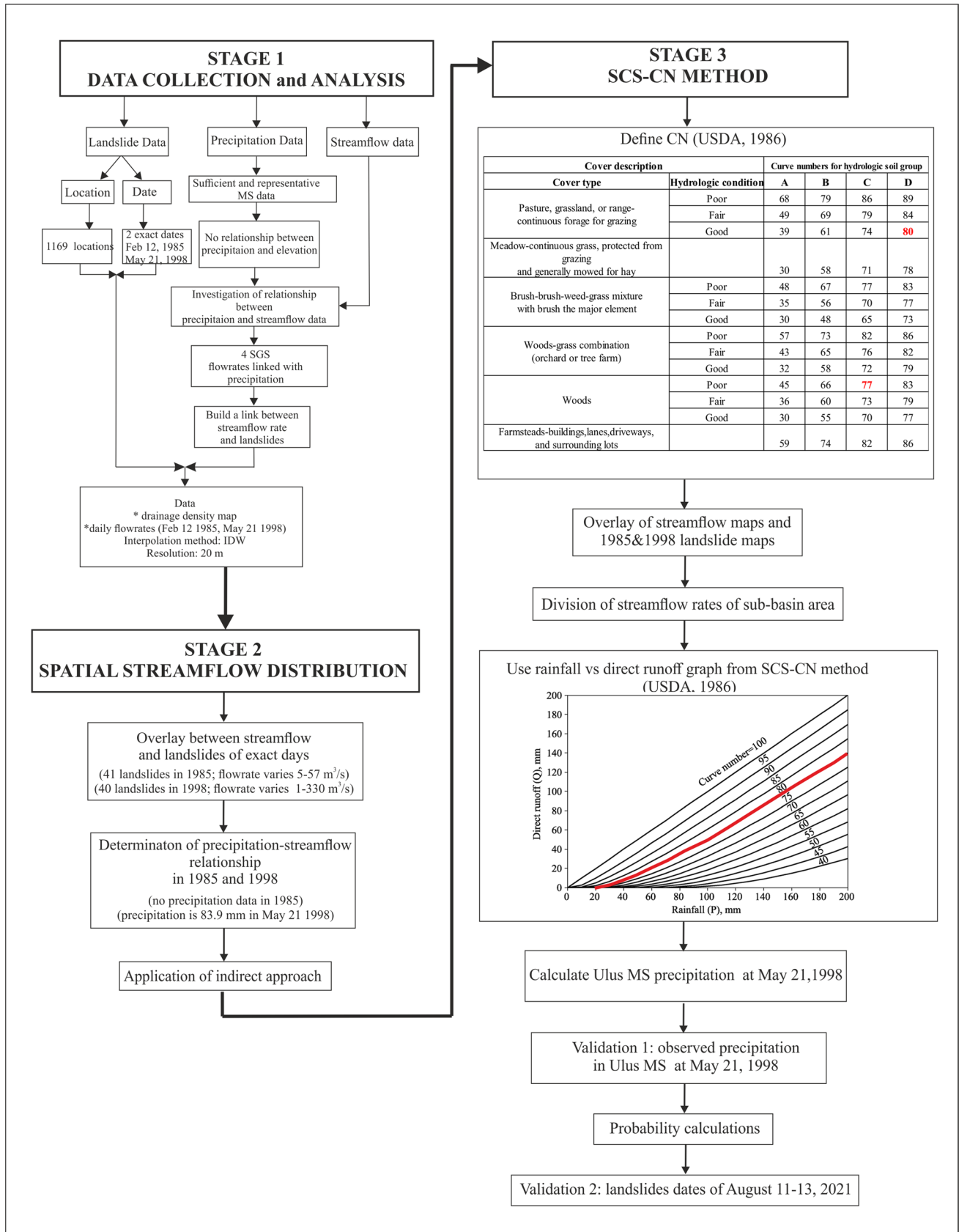
STAGE 1
DATA COLLECTION and ANALYSIS

Landslide Data

Location | Date

1169 locations

2 exact dates
Feb 12, 1985
May 21, 1998

Precipitation Data

Sufficient and representative MS data

No relationship between precipitaion and elevation

Investigation of relationship between precipitaion and streamflow data

4 SGS flowrates linked with precipitation

Build a link between streamflow rate and landslides

Streamflow data

Data
* drainage density map
*daily flowrates (Feb 12 1985, May 21 1998)
Interpolation method: IDW
Resolution: 20 m

STAGE 2
SPATIAL STREAMFLOW DISTRIBUTION

Overlay between streamflow and landslides of exact days

(41 landslides in 1985; flowrate varies 5-57 m³/s)
(40 landslides in 1998; flowrate varies 1-330 m³/s)

Determinaton of precipitation-streamflow relationship in 1985 and 1998

(no precipitation data in 1985)
(precipitation is 83.9 mm in May 21 1998)

Application of indirect approach

STAGE 3
SCS-CN METHOD

Define CN (USDA, 1986)

Cover description		Curve numbers for hydrologic soil group			
Cover type	Hydrologic condition	A	B	C	D
Pasture, grassland, or range-continuous forage for grazing	Poor	68	79	86	89
	Fair	49	69	79	84
	Good	39	61	74	**80**
Meadow-continuous grass, protected from grazing and generally mowed for hay		30	58	71	78
Brush-brush-weed-grass mixture with brush the major element	Poor	48	67	77	83
	Fair	35	56	70	77
	Good	30	48	65	73
Woods-grass combination (orchard or tree farm)	Poor	57	73	82	86
	Fair	43	65	76	82
	Good	32	58	72	79
Woods	Poor	45	66	**77**	83
	Fair	36	60	73	79
	Good	30	55	70	77
Farmsteads-buildings,lanes,driveways, and surrounding lots		59	74	82	86

Overlay of streamflow maps and 1985&1998 landslide maps

Division of streamflow rates of sub-basin area

Use rainfall vs direct runoff graph from SCS-CN method (USDA. 1986)

Calculate Ulus MS precipitation at May 21,1998

Validation 1: observed precipitation in Ulus MS at May 21, 1998

Probability calculations

Validation 2: landslides dates of August 11-13, 2021

Fig. 3 Methodological framework of the study

MS, approximately located in the central part of the study area, while Amasra, Bartın, and Kozcagiz MSs were outside of the study area. First, the precipitation–elevation relationship was investigated to determine the spatial distribution of the precipitation in the area. However, it has been revealed that microclimate has been observed in the region since the study area and its surroundings have been recharged by both marine and terrestrial precipitations. Since there was no precipitation–elevation relationship among Ulus MS and the other MSs around the area, only Ulus MS daily precipitation data at hand were considered for the 1966–2005 period (Fig. 4b). Although some data are missing, Ulus MS data have been considered for the analyses. Accordingly, the average annual precipitation (AAP) of Ulus MS is 1005.0 mm (st. dev. 180.6 mm). The highest precipitation was measured 1312.7 mm in 1967 and the lowest precipitation was 687.3 mm in 1986 (Fig. 4c). According to Ulus MS data, the rainy months in the study area are December and January, while the dry months are July and August.

Investigation of the landslides and their relationship with the terrain attributes such as drainage network characteristics is a crucial topic in landslide studies. Concerning drainage characteristics, the streams constituting the drainage system have significant effects on landslide initiation and landslide mechanism. Generally, streams not only erode slopes but also saturate the rock or soil materials, which adversely affect the slope stability and make the materials more prone to landsliding. In many landslide studies, the researchers consider drainage network-related parameters such as distance to drainage and drainage density. As Lima et al. (2022) stated, these two parameters have been revealed as the two of the most widely used landslide predictors (or conditioning parameters) in landslide assessments. The drainage density of the study area (see Fig. 2c) was used to build a link between the streamflow rate and the landslides in this study. First introduced by Horton (1932), it has been widely used in many hydrological studies and is determined by dividing the total length of streams within a drainage basin by the drainage area. For example, Melton (1957) has shown that for particular drainage basins, relationships exist between drainage density and both input (precipitation–effectiveness index) and output (runoff–intensity frequency). In a discussion of drainage density and streamflow, Carlston (1963) demonstrated a relationship between drainage density and average minimum monthly flow. Drainage density is related to watershed or physiographic characteristics such as relief ratio, rock type, and basin shape in addition to the input and output of the drainage basin system (Gregory and Walling 2010). Drainage density is directly related to geotechnical and hydrological characteristics (Ercanoglu 2005; Lima et al. 2022). As Sonker et al. (2021) stated, the drainage density is an inverse function of permeability. The less permeable the rock is, the less the infiltration of rainfall, which conversely tends to be concentrated in surface runoff. Since it was not possible to use the permeability of the lithological units, it was not wise to distribute this property in such a big region. As can be seen from the lithological map of the study area (see Fig. 2e), 93.4% of the study area was covered by the Ku and PTrc units. These units represent the flysch character, which stores the water, but does not transmit it. Since the drainage density was used to obtain streamflow map, as a weight factor, it allowed us to approach the spatial representation of the permeability of the lithological properties, which is explained in Stage 2.
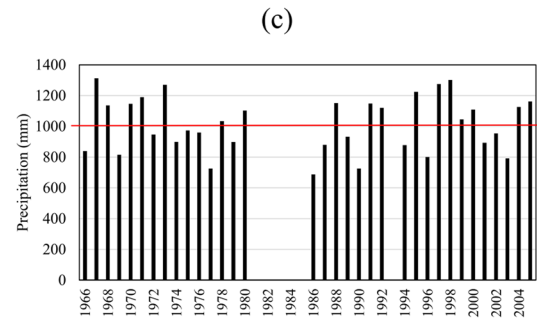
As for the SGS data, there are 4 SGSs within the study area. Three of them, namely D13A014, D13A039, and D13A049, were operated by the State Hydraulic Works (DSI), and the other one, namely 1331, was operated by the Electrical Works Survey Administration (EIE) (see Fig. 4a). Some data (DSI 2020) related to SGSs in the area are presented in Table 1 and Fig. 4d–g. Based on the data analysis of Ulus MS, the areal distribution of the precipitation could not be determined because the precipitation data of Ulus MS are not continuous (i.e., lack of data exists particularly in the landslide dates) and could not be considered as representative itself for the whole study area. Thus, in this study, the four above-mentioned SGS data were initially taken into consideration. Areal distribution of the streamflow data has been investigated by considering the flow rate values that will be linked to the precipitation as the landslide-triggering phenomenon for the next stage. Thus, in this stage, data related to four SGSs were analyzed. SGS 1331, located downstream of the study area, collects 100% of the streamflow occurred in the drainage area (see Fig. 4a). Percentages of flow rates measured in each SGS were calculated by proportioning the drainage areas of each SGS to the drainage area of 1331 SGS. According to this calculation among the SGSs in the study area, station number D13A049 is located on the tributary carries 10.1%, D13A039 24.4%, and station number D13A014 65.5% of the total flow, respectively (see Table 1).

The next stage (Stage 2) was to build a link between the streamflow rate and the landslides. Due to the insufficient precipitation data, a landslide–precipitation relationship could not be established. Therefore, this study has tried to link the streamflow and precipitation using an indirect method (SCS-CN method). To perform this method, the areal distribution of the streamflow rates has to be known. Since the two exact landslide dates were known (February 12, 1985 and May 21, 1998), 4 SGS streamflow data were used to interpolate the streamflow data. In order not to cause any scattering related to streamflow for the interpolation process, a different layer was needed to represent and obtain meaningful results. This need has been sourced from the fact that how the streamflow has spatially accumulated in the area. This problem has been solved by using
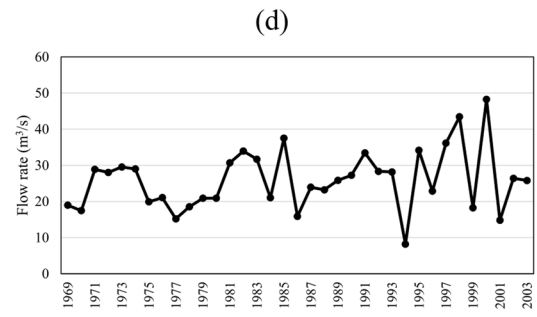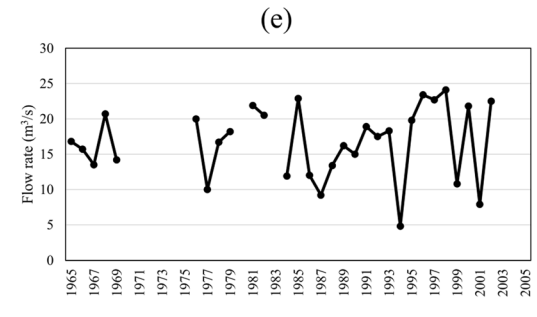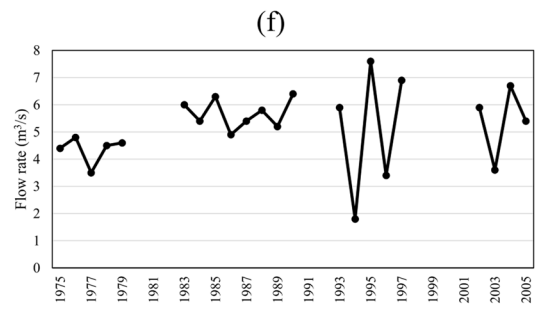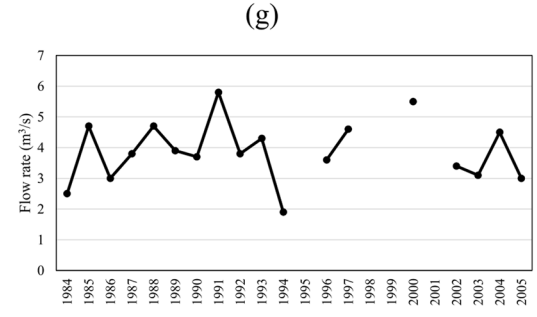
(a)

(b)
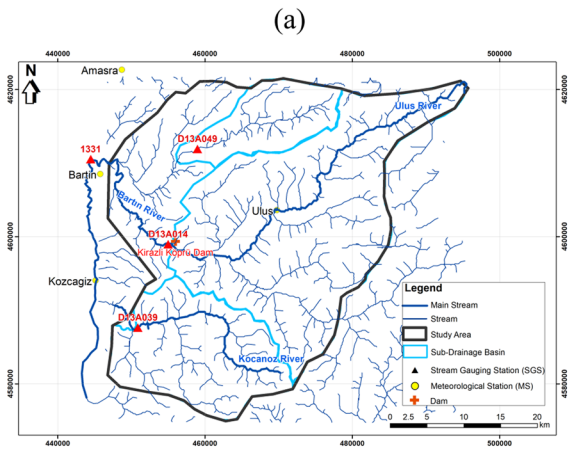
Year	MS	SGS			
	ULUS	1331	D13A014	D13A039	D13A049

☐ Data exist for MS
■ Data exist for SGS
☐ No data exist for both MS and SGS

(c)

(d)

(e)

(f)

(g)

◀**Fig. 4** Precipitation and streamflow data summary of the study area: **a** streams, locations of meteorological (MS) and stream gauging stations (SGS); **b** graphical representation of historical MS and SGS data; **c** annual precipitation data of Ulus MS; **d** annual streamflow data of 1331 SGS; **e** annual streamflow data of D13A014 SGS; **f** annual streamflow data of D13A039 SGS and **g** annual streamflow data of D13A049 SGS

the drainage density map, which has been normalized in [0, 1] interval (see Fig. 2c), and has been fed into the calculations as a weight factor in the Geostatistical IDW module of ArcGIS (version 10.6.1). This module uses the measured values surrounding the prediction location to predict a value for any unsampled location, based on the assumption that things that are close to one another are more alike than those that are farther apart (https://webhelp.esri.com/arcgisdesktop/) (ESRI 2023).

Areal streamflow distribution map with a 20 m resolution was used by considering the daily streamflow values measured in the SGSs on February 12, 1985 and May 21, 1998 (Fig. 5a and b). According to the distribution maps, the flow values in the study area were in the range of 0–208 m^3/s in 1985 and were between 0 and 882 m^3/s in 1998. The landslides that occurred on those days were also marked on the distribution maps. Accordingly, the flow value that created 41 landslides in 1985 varies between 5 and 57 m^3/s, while the flow that created 40 landslides in 1998 varies between 1 and 330 m^3/s. Thus, the dynamic of the precipitation–streamflow rate relationship was especially focused on these dates. Since there were no daily precipitation data at Ulus MS in 1985, precipitation data were not depicted on the 1985 graph, only flow rate values were used (Fig. 5a). It was stated in the records of 1985 that the landslides occurred on February 12. When daily flow rates are correlated with landslide events using 3 SGS data on landslide dates, it was revealed that the landslides occurred when the daily flow rate value was over 200 m^3/s (Fig. 6a), measured in 1331 SGS, located downstream of the drainage area. Similarly, according to the records of 1998 landslides occurred in the study area on May 21, and the flow rate reached 882 m^3/s at 1331 SGS on May 21, 1998. The precipitation was measured as 83.9 mm at Ulus MS on the same day. When the precipitation–flow rate graph of 1998 is examined (Fig. 6b), the flow rate in the stream has increased as it is expected, depending on the daily precipitation. However, the periods in which the flow rate is the highest in the stream will be after the consecutive rainy days.

Due to the lack of data and the existence of one MS in the area, the SCS-CN method has been considered as an alternative approach to reach the possible precipitation value triggered by the landslides as Stage 3 of the study. It is a widely used simple method for predicting direct runoff for a given rainfall event (Soulis and Valiantzas 2012). It has become a standard tool, in practice, for estimating an event-based rainfall–runoff response (Bartlett et al. 2016). In this method, the relationship between the direct runoff and rainfall could be estimated for different curve numbers (CN) representing various soil and land cover conditions. In the literature, with respect to landslides and hydrological modeling, this method has been successfully used and produced reliable results, particularly in data-scarce environments (Kannan et al. 2013; Zhang et al. 2015; Eshghizadeh et al. 2018; Guo et al. 2021; Natarajan and Radhakrishnan 2021; Obrike et al. 2021; Wu 2021; Bahmani et al. 2022; Peng et al. 2022; Zieher et al. 2022). Contrary to the general use of SCS-CN method, in this study, an approach to the determination of precipitation has been followed from the measured streamflow data. First, CN was determined from the land use map for the study area (see Fig. 2d). According to the SCS-CN method, the CN value of the forest areas covering 55.6% of the study area was 77, and the CN value of the agricultural areas covering 13.6% of the study area was 80. Then, using the flow rate maps represented in Fig. 5a and b, the 1985 and 1998 landslide locations were overlaid in the GIS platform. As a result of this process, the amount of flow rate forming each landslide was determined. Dividing the streamflow rate by the area of the sub-basin where a landslide is located, the surface runoff (Q) (mm) could be calculated. Finally, as can be seen from Fig. 3, rainfall versus direct runoff values have been determined by SCS-CN method. Accordingly, the precipitation that creates 0–110 mm runoff flow in the study area for 1985 (i.e., streamflow between 0 m^3/s and 208 m^3/s) varies between 20 and 165 mm. For the year 1998, the precipitation that created 0–478 mm runoff flow (i.e., streamflow between 0 m^3/s and 882 m^3/s) varies between 20 mm and 265 mm. In addition, the precipitation determined by the SCS-CN method for the location of Ulus MS was calculated as 190 mm for 1998. When these data have been compared with the daily precipitation data of May 1998, it has been revealed that it corresponds to the cumulative precipitation of 15 days (184 mm) on Ulus MS. Therefore, the amount of precipitation has been calculated as 190 mm that will create 218 m^3/s flow in 1998 the tributary on which Ulus MS is located. This result is encouraging in terms of the usability of the applied method because the amount of 190 mm precipitation calculated by SCS-CN method is very close to the 15-day cumulative precipitation value (i.e., 184 mm) measured at Ulus MS in 1998.

Results

This study, which is carried out in an area where landslides are known to be triggered by precipitation, focuses on an alternative approach based on streamflow data to the determination of the possible precipitation threshold values. A direct evaluation and/or modeling related to the precipitation

Table 1 Data related to SGSs within the study area

Station name (SGS)	Observation period	Drainage area (km²)	Station elevation (m, asl)	Annual average flow rate (m³/s)	Daily maximum flow rate (m³/s)
1331	1969–2003	1359	15	24.40	882
D13A014	1965–2002	890	80	16.29	600
D13A039	1975–2005	332	130	5.24	210
D13A049	1984–2005	137	230	3.80	220
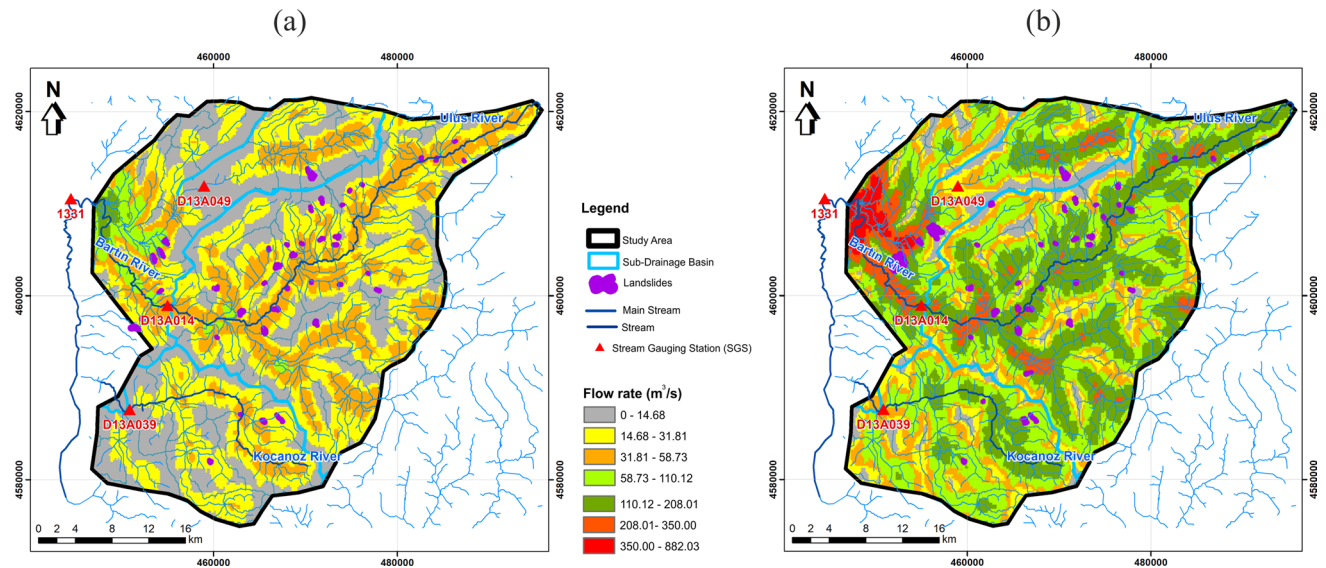
Fig. 5 Streamflow distribution maps of the study area for the landslide dates: **a** February 12, 1985 map and **b** May 21, 1998 map

that may trigger landslides could not be performed. Based on the data analyses, this situation was mainly sourced from deficiencies and/or uncertainties in landslide dates, precipitation and streamflow data (see Fig. 3). In addition, although more than 1000 landslides have been reported in the considered area, 2 exact days of landslide occurrences has been determined. Furthermore, it was not possible to establish a precipitation–elevation relationship in the study area because of the lack of precipitation data obtained from the other 3 MSs around the area. Thus, despite its data shortages, Ulus MS data, which are almost located in the central part of the study area, were considered. Nonetheless, it was tried to determine the possible precipitation threshold values that will trigger landslides using streamflow data and the SCS-CN method as an alternative approach that could be linked to the precipitation. In this regard, the determination of the possible threshold will be useful for future works such as landslide hazard and risk assessments. Since the essential purpose of this study is not to assess hazards or to produce a hazard map, no effort has been made on this issue.

For the future predictions, statistical models are widely used in such a study. Statistical analyses are frequently used

in natural disaster assessment and modeling, and probability calculations can be applied to possible disaster types in the future. With the help of the calculated probability values, it is possible to assess the hazard potential of the considered disaster. The probability value is calculated as the probability of exceeding the threshold in the data sets or a selected value (such as precipitation, or streamflow value). However, due to the lack and/or uncertainties in the data, researchers present different scenarios to the users and/or decision-makers in the hazard assessments. Triggering factor analyses could be applied with statistical distribution models and they can be carried out based on the assumption that the data are in continuous format. In such approaches, events are assumed to be random. To obtain temporal probabilities of landslide occurrences, there are generally two ways to perform some statistical analyses on the existing historical data in the literature. One is to perform the analyses considering some statistical distributions such as binomial or Poisson (Crovelli 2000) using complete multitemporal data for the periods between landslides and triggering events. The other one is to consider particularly the long-term hydrological data analyzing the exceedance probability using extreme

Fig. 6 Distribution of streamflow and precipitation data at the Ulus MS and SGS(s): **a** for 1985 and **b** for 1998
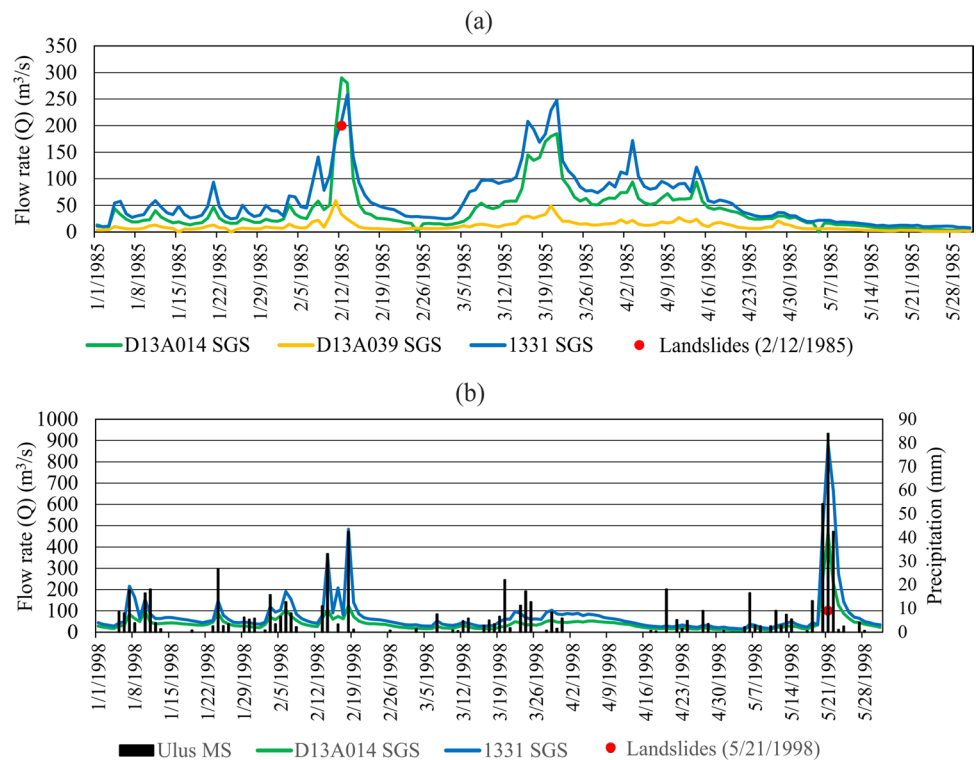
value analysis, a method that makes use of historical data to infer the probabilities of future extremes. In other words, it becomes possible to calculate the probability of a specific value that will be exceeded in a given future period. It has recently been used in relation to the extreme hydrological events occurred in a given period to calculate the temporal probabilities of the triggered landslides in the landslide literature (e.g., Xiao et al. 2020; Bulti et al. 2021; Ciccarese et al. 2021; Lin et al. 2021; Putty et al. 2021; Rana and Babu 2022; Sheng et al. 2022; Tehrani et al. 2022; Zhu et al. 2022). The maximum and/or the minimum of several extremes of the years could be modeled by using the Gumbel distribution (Gumble 1954) as given in the Eqs. 1 and 2 for probability density function ($f(x)$) and cumulative distribution function ($F(x)$), respectively:

$$f(x) = \frac{1}{\sigma} \exp\left(-z - \exp\left(-z\right)\right), \tag{1}$$

$$F(x) = \exp\left(-\exp\left(-z\right)\right), \tag{2}$$

where $z \equiv \left((x - \mu)/\sigma\right)$, σ is the continuous scale parameter ($\sigma > 0$), μ is the continuous location parameter in $-\infty < x < +\infty$ domain. To obtain the probability of exceedance to cause landslides in the study area, monthly average maximum flow rates of 1331 SGS containing data for the period of 1969–2003 (Table 2) were used (average flow rate: 72.85 m³/s, st. dev.: 28.87 m³/s). Before

calculating the probability of exceedance, firstly, probability density and cumulative density functions were obtained by using the related data tabulated in Table 2 (Fig. 7a and b). Then, the goodness of fit of the Gumbel distribution was tested by Kolmogorov–Smirnov (KS) test using a computer code, called EasyFit (Ver. 5.5). The KS test is a nonparametric test whether the considered data follow a null hypothesis (H_0) or not (H_1) at different significance levels. Based on the different significance levels ranging from 0.8 to 0.99, all H_0 hypotheses were accepted and were statistically meaningful based on these analyses. Thus, it was decided to use the Gumbel distribution for calculating the exceedance probabilities of the streamflow data by the same computer code. Next, considering different possible streamflow rates (see Fig. 5) that occurred in the study area on the landslide dates and their corresponding precipitation values calculated by SCS-CN method were tabulated in Table 3. In addition, probabilities (p) of the streamflow values were calculated based on the Gumbel model (see Table 3). In addition, for future predictions, the probability of exceedance (PoE(N)) over N years of the considered streamflow rates was also calculated using Eq. 3 below:

$$PoE(N) = 1 - (1 - p)^N. \tag{3}$$

All these calculated probabilities for different streamflow rates are tabulated in Table 3. It should be noted that

Table 2 Montly average maximum streamflow rates of 1331 SGS for the period of 1969–2003

Year	Flow rate (m³/s)	Year	Flow rate (m³/s)
1969	67.4	1987	96.4
1970	64.0	1988	56.5
1971	77.5	1989	71.4
1972	96.7	1990	77.8
1973	54.4	1991	87.0
1974	86.3	1992	79.5
1975	51.0	1993	66.9
1976	55.4	1994	19.2
1977	44.7	1995	91.2
1978	49.1	1996	49.6
1979	61.9	1997	99.7
1980	63.7	1998	127.0
1981	80.8	1999	58.1
1982	79.6	2000	175
1983	86.5	2001	48.5
1984	34.0	2002	74.4
1985	106.0	2003	66.1
1986	46.6		

different streamflow values were considered for the probability calculations in Table 3. Probability calculations were made for different periods ranging from 5 to 100 years by considering the several streamflow rates and their corresponding precipitation values.

It is certainly necessary to verify the methodological approach and the determined threshold values by considering the streamflow, precipitation and landslide-related parameters taken into consideration for actual conditions and future predictions. For the verification process, Bartın AFAD provincial authorities were contacted and information was asked whether there were landslides or not in the region after any precipitation in recent years in addition to archive studies. In line with the information received from the officials, press sources, and archive records, it was revealed that there were many landslides and floods in the region, which also included the study area, on August 11–13, 2021. After this stage, streamflow and precipitation data were obtained to cover the dates in 2021 (Fig. 8). For the year 2021 data in Fig. 8, there were 3 significant peaks with respect to landslide dates, streamflow and precipitation data. In these data sets since the beginning of 2021, either there was no official landslide record or the occurred landslides were outside of the study area for Peak 1 and Peak 2 regions. As for the landslide dates of August 11–13, 2021 (Peak 3 region), based on the official landslide records located in the close vicinity of Kumluca, Ulus, and Abdipaşa districts in the study area (see Fig. 1), many roads were closed and bridges were damaged, and
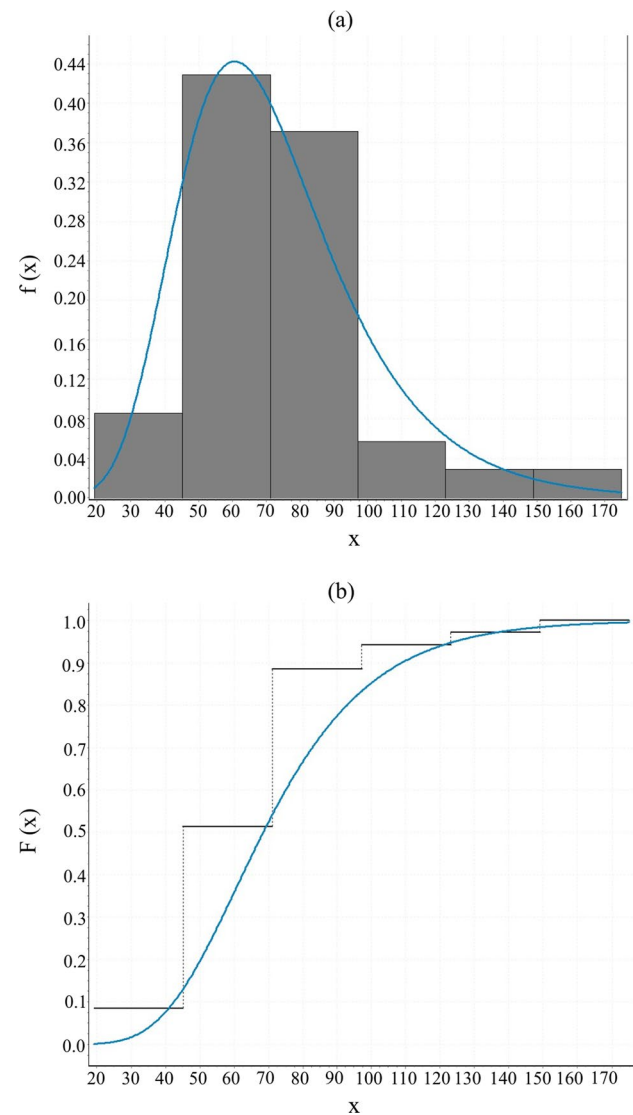

Fig. 7 Schematical representation of streamflow data by Gumbel distribution: **a** probability density function and **b** cumulative distribution function

one person killed due to landslides. On the landslide day, the daily precipitation was 90 mm and the antecedent cumulative precipitation for 15 days was 169.4 mm at Ulus MS. When compared with the 1998 landslide events, the daily precipitation of the landslide day was 83.9 mm and the antecedent cumulative precipitation for 15 days was 184 mm at the same MS, respectively. Thus, it could be considered that more than 80 mm of daily precipitation and cumulative precipitation of any consecutive days of 160 mm could be selected as the threshold values that may trigger the landslides in the region. To remain on the safe side, values lower than those determined in the landslide dates were chosen since these values were obtained using an indirect analysis method (i.e., SCS-CN method).

Table 3 Calculated probabilities of the considered streamflow rates, corresponding precipitation values, and periods

Streamflow (m³/s)	25	50	75	100	125	150	175
Precipitation (mm)	57	76	102	119	138	165	184
p (Gumbel)	0.99	0.80	0.40	0.15	0.05	0.02	0.01
PoE (5 years)	1.0000	0.9997	0.9222	0.5563	0.2262	0.0961	0.0490
PoE (10 years)	1.0000	1.0000	0.9940	0.8031	0.4013	0.1829	0.0956
PoE (25 years)	1.0000	1.0000	1.0000	0.9828	0.7226	0.3965	0.2222
PoE (50 years)	1.0000	1.0000	1.0000	0.9997	0.9231	0.6358	0.3950
PoE (100 years)	1.0000	1.0000	1.0000	1.0000	0.9941	0.8674	0.6340

Fig. 8 Streamflow and precipitation data at 1331 SGS and Ulus MS in 2021
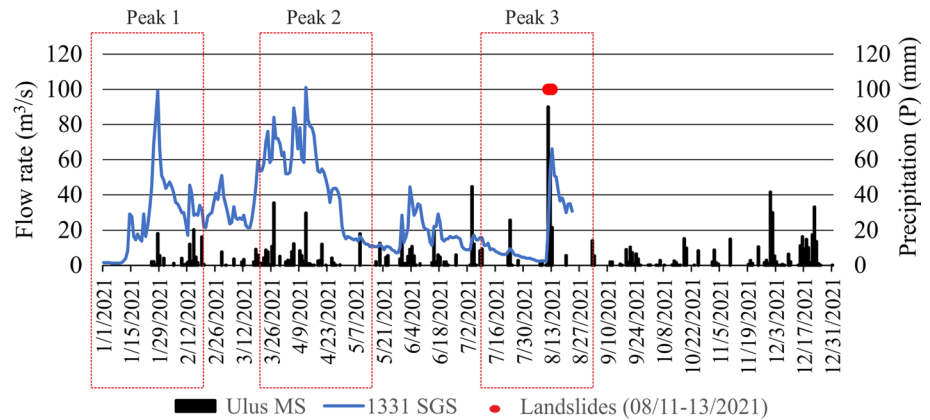
An assessment should also be made in terms of streamflow values on which the calculations are based. According to the streamflow data in the study area, the flow values range from 0 m³/s to 208 m³/s (in 1985) and from 0 m³/s to 882 m³/s (in 1998), which is an extreme event. On the other hand, in 2021, these values are between 0 m³/s and 99.2 m³/s (at which the 1331 SGS located and downstream of the study area). In addition, as can be seen from Fig. 8, 1331 SGS was damaged by the flood in August 2021 and no flow measurement was made after that date. Although there is a similarity between the calculated precipitation values, it can be thought that there could be a decrease in the streamflow values in 2021. The main reason for this situation is sourced from the Kirazlı Köprü dam (see Fig. 4a), which was initiated to be built in 1999 for irrigation, water supply, energy and flood control purposes and started to collect water in its reservoir since 2018.

Another significant issue that could be considered in the current study is whether there was a significant change in the land use parameter considered in the SCS-CN method for two different periods. As mentioned before, the land use map was the product of the year 2006 by CORINE. When applying the SCS-CN method for the year 2021, it was also tested how much land use change happened in the area. To evaluate the change in land use, available data set of the study area for the year 2018, the closest data set to the year of 2021, by CORINE was obtained. Then, the change in the study area was evaluated by subtracting the land use maps of the two periods (i.e., years from 2018 to 2006) (Fig. 9a and Fig. 9b). According to the results of this subtraction, it was revealed that the land use change was only 2.2% throughout the study area (Fig. 9c), particularly in the southeastern part. The changes were revealed from agricultural areas to forest, and/or from woodlands to forest. Thus, the difference in land use change between two different temporal periods was assumed negligible and the SCS-CN method was applied to the selected area. One of the most important issues here is that the area taken into consideration shows rural settlement characteristics and there is no significant change in terms of industry and urbanization. Although this approach has limitations, obtaining reasonable and consistent results with other data groups has been accepted as an indicator of the applicability of this method in data-scarce regions with respect to landslides.

According to the determined precipitation thresholds, the most important outcome of the current study is that the calculated numerical probability values have turned into a reality in the study area. For example, while the probability of 165 mm precipitation with a 50-year recurrence period in 25 years is approximately 39% (see Table 3), it could be considered that this probability occurs within 23 years when the 1998 and 2021 landslide dates are considered.
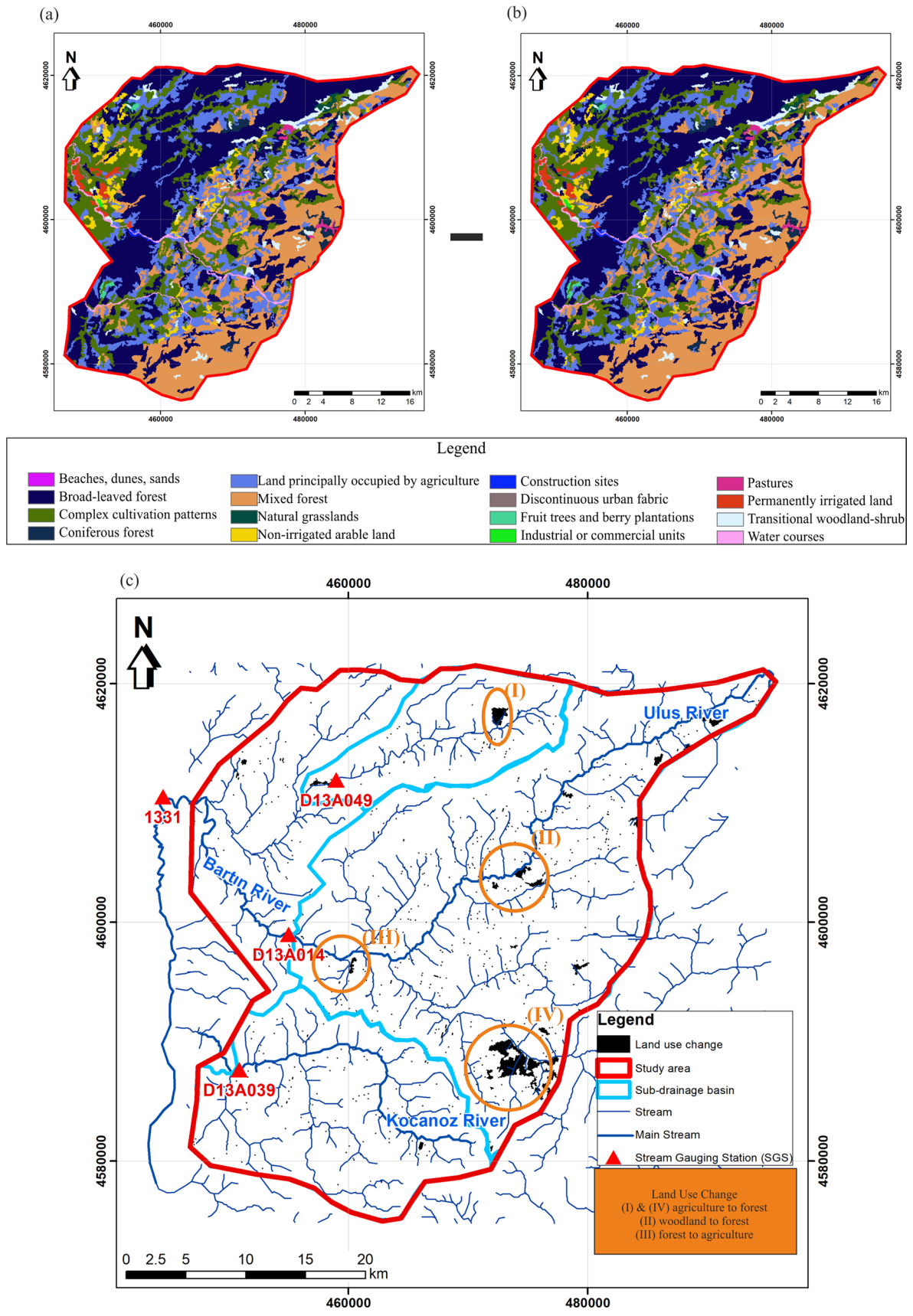
Fig. 9 Land use maps of the study area: **a** for the year of 2018; **b** for the year of 2006 and **c** the difference between the years of 2018 and 2006

Discussion and conclusion

The long-term data of 4 different SGSs in the study area were evaluated together with the existing landslide archives and precipitation data. By calculating how much streamflow in the study area was measured by each SGS, areal flow distribution maps were produced for the dates of February 12, 1985, and May 21, 1998, on which the 81 landslides occurred. While the distribution map of 1985 took values between 0 and 208 m^3/s, the 1998 map took values between 0 and 882 m^3/s. After determining the spatial flow distribution, the precipitation equivalent of the flow was determined. For this, surface runoff was calculated in meters by proportioning the volumetrically measured flow value to the drainage areas. In this study, the CN value was determined for the study area using the SCS-CN method and precipitation was calculated using the runoff–precipitation graph from the runoff in 1985 and 1998 (0–110 mm and 0–478 mm, respectively). Accordingly, the precipitation in 1985 was determined between 0 mm and 165 mm, and for the year 1998, it was between 0 mm and 265 mm. To check the accuracy of the calculated precipitation values, the daily precipitation of Ulus MS in May 1998 was used. On the May 21, 1998, flow distribution map, the flow at the location of Ulus MS was 218 m^3/s and the corresponding precipitation was calculated as 190 mm by the SCS-CN method. In addition, the 15-day antecedent cumulative precipitation value of Ulus MS before May 21, 1998, was 184 mm. The closeness of these two values suggested that the triggering precipitation threshold for landslides could be approached by the applied methodological steps. It has been revealed that the precipitation and the resulting streamflow, especially in 1998, have a value of more than a 100-year recurrence period. Unfortunately, the same methodological calculation steps could not be performed for the February 12, 1985, landslides because the daily precipitation was not measured in Ulus MS on that day.

Although the obtained results and the validations of both numerical and the realized probabilities are promising, of course, the applied methodology in the study has some limitations and uncertainties related to available data. Even though these issues were frequently addressed in the literature (e.g., Erener and Düzgün 2013; Kim et al. 2021), the researchers must make some assumptions or work with the data they have. For example, in the Erener and Düzgün (2013) study, partially covering the SW part of the current study area and using the Bartın MS data, they had to use one MS data to assess the landslide hazard. In addition, those authors have assessed the critical precipitation thresholds on daily and different antecedent days in their study as 63 mm (daily) and 266 mm (antecedent 20 days). Although the indirectly calculated daily precipitation (60 mm) in the current study was following the results of Erener and Düzgün (2013) study, the result of the antecedent 20 days of that study was 266 mm. These differences were considered reasonable because the areal extents, topographical and climatological conditions were not the same in addition to the calculation methods.

In addition, this study has not considered the streamflow–elevation relation (slope along streamflow) issue, which could be considered as common in such a study. For example, Hunsaker et al. (2012) highlighted the meteorological, and topographic characteristics typical of mountainous terrain produce strong contrasts in the timing, magnitude, and frequency of streamflow events within different elevation zones. Few studies consider how this elevation-driven heterogeneity complicates our understanding of elevation–streamflow patterns (Tennant et al. 2015). However, the study area is in a data-scarce region, but it a highly prone to landslides. There are only 4 SGS stations that are mostly located on the west side of the area. When the topographical and geographical conditions of the study area are considered, it could be seen that the NE part of the study area relatively represents the highest elevations and the precipitation. Thus, streams in this NE part are mostly perennial and it will not be possible to observe continuous stream flow.

Kirazlı Köprü dam (see Fig. 4a) is continuously derivating the surface water to the irrigation channels. Therefore, in the future, it does not seem highly possible to release the water from the dam gates and/or by the dam operator. In addition, since the volume of the reservoir was designed for the previously occurred floods, landslides would be possible downstream of the dam if higher streamflows occur than those of the designed values.

Notwithstanding the data deficiencies and uncertainties, this study is an example of the usability of an indirect method for approaching the possible precipitation thresholds in a data-scarce region. While the SCS-CN method is frequently used in determining the runoff using mainly precipitation data, it has been introduced as an approach to calculate the probable precipitation forming the runoff. The presence of many MSs that can represent the areal precipitation in areas where the precipitation regime differs, the continuous and long-term data measurement will facilitate the determination of the precipitation threshold(s) that will trigger the landslides. In addition, high-resolution flow distribution maps can be made with more SGSs to be built on the stream tributaries in such an area. In addition to areal precipitation distribution and flow observations, further research on the hydrogeological (e.g., porosity, specific yield, and specific retention) and/or hydrological characteristics in such landslide-prone areas is also important. Thus, by increasing the data quality and the resources in the future, it will be possible to minimize the damages and losses sourced

from the natural hazards, not only in the study area but also throughout the Black Sea region of Türkiye, where landslides and floods frequently occur.

Declarations

Conflict of interest The authors declare no competing interests. Administrative conflicts.

Ethics approval Not applicable.

Consent to participate Not applicable.

Consent for publication Not applicable.

References

AFAD (2022) Ministry of Interior Disaster and Emergency Management Presidency https://www.afad.gov.tr/ (01.04.2022)

Althuwaynee OF, Pradhan B, Ahmad N (2015) Estimation of rainfall threshold and its use in landslide hazard mapping of Kuala Lumpur metropolitan and surrounding areas. Landslides 12:861–875. https://doi.org/10.1007/s10346-014-0512-y

Ávila FF, Alvalá RC, Mendes RM, Amore DJ (2021) The influence of land use/land cover variability and rainfall intensity in triggering landslides: a back-analysis study via physically based models. Nat Hazards 105(1):1139–1161. https://doi.org/10.1007/s11069-020-04324-x

Bahmani F, Fattahi MH, Sabzevari T, Haghighi AT, Talebi A (2022) Spatial–temporal analysis of landslides in complex hillslopes of catchments using Dynamic Topmodel. Acta Geophys 70:1417–1432. https://doi.org/10.1007/s11600-022-00786-8

Bai S, Wang J, Thiebes B, Cheng C, Yang Y (2014) Analysis of the relationship of landslide occurrence with rainfall: a case study of Wudu County, China. Arab J Geosci 7:1277–1285. https://doi.org/10.1007/s12517-013-0939-9

Bartlett MS, Parolari AJ, McDonnell JJ, Porporato A (2016) Beyond the SCS-CN method: a theoretical framework for spatially lumped rainfall-runoff response. Water Resour Res 52:4608–4627. https://doi.org/10.1002/2015WR018439

Bhandary NP, Dahal RK, Timilsina M, Yatabe R (2013) Rainfall event-based landslide susceptibility zonation mapping. Nat Hazards 69(1):365–388. https://doi.org/10.1007/s11069-013-0715-x

Brabb EE (1991) The World Landslide Problem. Episodes https://doi.org/10.18814/epiiugs/1991/v14i1/008

Brunetti MT, Peruccacci S, Rossi M, Luciani S, Valigi D, Guzetti F (2010) Rainfall thresholds for the possible occurrence of landslides in Italy. Nat Hazards Earth Syst Sci 10(3):447–458. https://doi.org/10.5194/nhess-10-447-2010

Bulti DT, Abebe BG, Biru Z (2021) Climate change–induced variations in future extreme precipitation intensity–duration–frequency in flood-prone city of Adama, central Ethiopia. Environ Monit Assess. https://doi.org/10.1007/s10661-021-09574-1

Carlston CW (1963) Drainage density and streamflow: U. S. Geol. Survey Prof. Paper, 422-C, 8 pp

Ciccarese G, Mulas M, Corsini A (2021) Combining spatial modelling and regionalization of rainfall thresholds for debris flows hazard mapping in the Emilia-Romagna Apennines (Italy). Landslides 18:3513–3529. https://doi.org/10.1007/s10346-021-01739-w

CORINE (2006&2018) CORINE Land Cover. https://land.copernicus.eu/pan-european/corine-land-cover (14.09.2022)

CRED (2020) Natural disasters 2019: Now is the time to not give up. Centre for Research on the Epidemiology of Disasters (CRED), 8 p. https://www.preventionweb.net/publication/natural-disasters-2019-now-time-not-give (19.08.2022)

Crovelli RA (2000) Probability models for estimation of number and costs of landslides open-file report 00–249

Das P, Patwa D, Vishnu G, Bharat TV (2022) Influencing factors on the simulation of rainfall-induced landslide prediction based on case study. Bull Eng Geol Environ. https://doi.org/10.1007/s10064-022-02682-3

DSI (2020) State Hydraulic Works, Annual flow rate observations https://www.dsi.gov.tr/Sayfa/Detay/744 (04.11.2020)

Du W, Pan TC (2020) Probabilistic seismic hazard assessment for Singapore. Nat Hazards 103:2883–2903. https://doi.org/10.1007/s11069-020-04107-4

Ercanoglu M (2005) Landslide susceptibility assessment of SE Bartin (West Black Sea region, Türkiye) by artificial neural networks. Nat Hazards Earth Syst Sci. https://doi.org/10.5194/nhess-5-979-2005

Ercanoglu M, Kasmer O, Temiz N (2008) Adaptation and comparison of expert opinion to analytical hierarchy process for landslide susceptibility mapping. Bull Eng Geol Environ. https://doi.org/10.1007/s10064-008-0170-1

Erener A, Düzgün HSB (2012) Landslide susceptibility assessment: What are the effects of mapping unit and mapping method? Environ Earth Sci 66:859–877. https://doi.org/10.1007/s12665-011-1297-0

Erener A, Düzgün HBS (2013) A regional scale quantitative risk assessment for landslides: Case of Kumluca watershed in Bartin, Türkiye. Landslides 10:55–73. https://doi.org/10.1007/s10346-012-0317-9

Eshghizadeh M, Talebi A, Dastorani MT (2018) A modified LAPSUS model to enhance the effective rainfall estimation by SCS-CN

method. Water Resour Manag 32:3473–3487. https://doi.org/10.1007/s11269-018-2002-9

ESRI (2023) ArcGIS Desktop Help, How to Inverse Distance Weighted (IDW) interpolation works https://webhelp.esri.com/arcgisdesktop/ (19.12.2023)

Fan X, Scaringi G, Xu Q, Zhan W, Dai L, Li Y, Pei X, Yang Q, Huang R (2018) Coseismic landslides triggered by the 8th August 2017 M s 7.0 Jiuzhaigou earthquake (Sichuan, China): factors controlling their spatial distribution and implications for the seismogenic blind fault identification. Landslides. https://doi.org/10.1007/s10346-018-0960-x

Firincioglu BS, Ercanoglu M (2021) Insights and perspectives into the limit equilibrium method from 2D and 3D analyses. Eng Geol. https://doi.org/10.1016/j.enggeo.2020.105968

Fowze JSM, Bergado DT, Soralump S, Voottipreux P, Dechasakulsom M (2012) Rain-triggered landslide hazards and mitigation measures in Thailand: From research to practice. Geotext Geomembranes 30:50–64. https://doi.org/10.1016/j.geotexmem.2011.01.007

Ghosh TK, Jakobsen F, Joshi M, Pareta K (2019) Extreme rainfall and vulnerability assessment: case study of Uttarakhand rivers. Nat Hazards 99:665–687. https://doi.org/10.1007/s11069-019-03765-3

Glade T, Crozier M, Smith P (2000) Applying probability determination to refine landslide-triggering rainfall thresholds using an empirical "'Antecedent daily rainfall model.'" Pure appl Geophys 157(68):1059–1079

Gregory KJ, Walling DE (2010) The variation of drainage density within a catchment. Hydrol Sci Jrnl 13(2):61–68. https://doi.org/10.1080/02626666809493583

Gumble EJ (1954) Statistical theory of extreme values and some practical applications. U.S. Dept. of Commerce, National Bureau of Standards Applied Mathematics Series, 33

Guo X, Li Y, Chen X, Zhang J, Sun Y (2021) Variation of debris flow/flood formation conditions at the watershed scale in the Wenchuan Earthquake area. Landslides 18:2427–2443. https://doi.org/10.1007/s10346-021-01644-2

Guzzetti F, Peruccacci S, Rossi M, Stark CP (2007) Rainfall thresholds for the initiation of landslides in central and southern Europe. Meteorol Atmos Phys 98(3–4):239–267. https://doi.org/10.1007/s00703-007-0262-7

Guzzetti F, Peruccacci S, Rossi M, Stark CP (2008) The rainfall intensity-duration control of shallow landslides and debris flows: an update. Landslides. https://doi.org/10.1007/s10346-007-0112-1

Hong M, Kim J, Jeong S (2018) Rainfall intensity-duration thresholds for landslide prediction in South Korea by considering the effects of antecedent rainfall. Landslides 15:523–534. https://doi.org/10.1007/s10346-017-0892-x

Horton RE (1932) Drainage basin characteristics. Transact Am Geophys Union 13:350–361

Hunsaker CT, Whitaker TW, Bales RC (2012) Snowmelt runoff and water yield along elevation and temperature gradients in California's Southern Sierra Nevada. J Am Water Resour Assoc 48(4):667–678

Jakob M, Weatherly H (2003) A hydroclimatic threshold for landslide initiation on the North Shore Mountains of Vancouver, British Columbia. Geomorphology 54:137–156. https://doi.org/10.1016/S0169-555X(02)00339-2

Jibson RW, Harp EL (2016) Ground motions at the outermost limits of seismically triggered landslides. Bull Seismol Soc Am. https://doi.org/10.1785/0120150141

Kannan M, Saranathan E, Anabalagan R (2013) Landslide vulnerability mapping using frequency ratio model: A geospatial approach in Bodi-Bodimettu Ghat section, Theni district, Tamil Nadu, India. Arab J Geosci 6:2901–2913. https://doi.org/10.1007/s12517-012-0587-5

Keles F, Nefeslioglu HA (2021) Infinite slope stability model and steady-state hydrology-based shallow landslide susceptibility evaluations: The Guneysu catchment area (Rize, Türkiye). Catena. https://doi.org/10.1016/j.catena.2021.105161

Kim H, Lee JH, Park HJ, Heo JH (2021) Assessment of temporal probability for rainfall-induced landslides based on nonstationary extreme value analysis. Eng Geol. https://doi.org/10.1016/j.enggeo.2021.106372

Kim Y, Rahardjo H, Nistor MM, Satyanaga A, Leong EC, Sham AWL (2022) Assessment of critical rainfall scenarios for slope stability analyses based on historical rainfall records in Singapore. Environ Earth Sci. https://doi.org/10.1007/s12665-021-10160-4

Lateh H, Tay LT, Khan YA, Kamil AA, Azizat N (2013) Prediction of landslide using rainfall intensity-duration threshold along East-West Highway, Malaysia. Casp J Appl Sci Res 2:124–133

Leonarduzzi E, Molnar P (2020) Deriving rainfall thresholds for landsliding at the regional scale: Daily and hourly resolutions, normalisation, and antecedent rainfall. Nat Hazards Earth Syst Sci 20:2905–2919. https://doi.org/10.5194/nhess-20-2905-2020

Li WY, Liu C, Scaioni M, Sun WW, Chen Y, Yao DJ, Chen S, Hong Y, Zhang KH, Cheng GD (2017) Spatio-temporal analysis and simulation on shallow rainfall-induced landslides in China using landslide susceptibility dynamics and rainfall I-D thresholds. Sci China Earth Sci 60:720–732. https://doi.org/10.1007/s11430-016-9008-4

Lima P, Steger S, Glade T, Murillo-Garcia FG (2022) Literature review and bibliometric analysis on data-driven assessment of landslide susceptibility. J Mt Sci 19(6):1670–1698. https://doi.org/10.1007/s11629-021-7254-9

Lin W, Yin K, Wang N, Xu Y, Guo Z, Li Y (2021) Landslide hazard assessment of rainfall-induced landslide based on the CF-SINMAP model: a case study from Wuling Mountain in Hunan Province, China. Nat Hazards 106:679–700. https://doi.org/10.1007/s11069-020-04483-x

Lombardo L, Bakka H, Tanyas H, van Westen C, Mai PM, Huser R (2019) Geostatistical modeling to capture Seismic-shaking patterns from earthquake-ınduced landslides. J Geophys Res Earth Surf. https://doi.org/10.1029/2019JF005056

Mandal S, Maiti R (2013) Assessing the triggering rainfall-induced landslip events in the Shivkhola Watershed of Darjiling Himalaya, West Bengal. Eur J Geography 4(3):21–37

Marra F (2019) Rainfall thresholds for landslide occurrence: systematic underestimation using coarse temporal resolution data. Nat Hazards. https://doi.org/10.1007/s11069-018-3508-4

Melillo M, Brunetti MT, Peruccacci S, Gariano SL, Guzzetti F (2016) Rainfall thresholds for the possible landslide occurrence in Sicily (Southern Italy) based on the automatic reconstruction of rainfall events. Landslides 13:165–172. https://doi.org/10.1007/s10346-015-0630-1

Melton MA (1957) An Analysis of the Relations among the Elements of Climate, Surface Properties, and Geomorphology, Technical Report 11. Department of Geology, Columbia University, New York

MGM (2022) State Meteorological Service of Türkiye MEVBIS, Meteorological data information and sales system. https://mevbis.mgm.gov.tr/mevbis/ui/index.html#/Workspace (15.03.2022)

Natarajan S, Radhakrishnan N (2021) Simulation of rainfall–runoff process for an ungauged catchment using an event-based hydrologic model: a case study of koraiyar basin in Tiruchirappalli City, India. J Earth Syst Sci. https://doi.org/10.1007/s12040-020-01532-8

Obrike SE, Barr SL, Miller PE, Anudu GK (2021) Engineered slope failure susceptibility modelling using high spatial resolution

geospatial data. Bull Eng Geol Environ 80:7361–7384. https://doi.org/10.1007/s10064-021-02413-0

Peng T, Chen N, Hu G, Tian S, Ni H, Huang L, Yang X, Zhao A (2022) Failure mechanism of Dege landslide in western China, March 2021: the loess interlayer and multiple water resources. Landslides 19:2189–2197. https://doi.org/10.1007/s10346-022-01910-x

Putty MRY, Prithviraj BN, Kumar PN, Nithish MG, Giri G, Chandramouli PN (2021) An insight into the hydrological aspects of landslides of 2018 in Kodagu, South India. Landslides 18:1597–1610. https://doi.org/10.1007/s10346-020-01589-y

Ramos-Cañón AM, Prada-Sarmiento LP, Trujillo-Vela MG, Macías JP, Santos-R AC (2016) Linear discriminant analysis to describe the relationship between rainfall and landslides in Bogotá Colombia. Landslides 13(4):671–681. https://doi.org/10.1007/s10346-015-0593-2

Rana H, Babu GLS (2022) Regional back analysis of landslide events using TRIGRS model and rainfall threshold: an approach to estimate landslide hazard for Kodagu, India. Bull Eng Geol Environ. https://doi.org/10.1007/s10064-022-02660-9

Sassa K, Fukuoka H, Wang F, Wang G (2007) Landslides induced by a combined effect of earthquake and rainfall. Prog Landslide Sci. https://doi.org/10.1007/978-3-540-70965-7_14

Sheng Y, Li Y, Xu G, Li Z (2022) Threshold assessment of rainfall-induced landslides in Sangzhi County: statistical analysis and physical model. Bull Eng Geol Environ. https://doi.org/10.1007/s10064-022-02890-x

Sonker I, Tripathi JN, Singh AK (2021) Landslide susceptibility zonation using geospatial technique and analytical hierarchy process in Sikkim Himalaya. Quat Sci Adv 4:100039. https://doi.org/10.1016/j.qsa.2021.100039

Soulis KX, Valiantzas JD (2012) SCS-CN parameter determination using rainfall-runoff data in heterogeneous watersheds-the two-CN system approach. Hydrol Earth Syst Sci. https://doi.org/10.5194/hess-16-1001-2012

Tanyas H, Lombardo L (2020) Completeness Index for Earthquake-Induced Landslide Inventories. Eng Geol. https://doi.org/10.1016/j.enggeo.2019.105331

Tehrani FS, Calvello M, Liu Z, Zhang L, Lacasse S (2022) Machine learning and landslide studies: recent advances and applications. Nat Hazards. https://doi.org/10.1007/s11069-022-05423-7

Tennant CJ, Crosby BT, Godsey SE (2015) Elevation-dependent responses of streamflow to climate warming. Hydrol Process 29:991–1001. https://doi.org/10.1002/hyp.10203

Tien Bui D, Pradhan B, Lofman O, Revhaug I, Dick ØB (2013) Regional prediction of landslide hazard using probability analysis of intense rainfall in the Hoa Binh province. Vietnam Nat Hazards 66:707–730. https://doi.org/10.1007/s11069-012-0510-0

USDA (1986) Urban Hydrology for Small Watersheds TR-55. Natural Resources Conservation Service: Retrieved from https://www.nrcs.usda.gov/Internet/FSE_DOCUMENTS/stelprdb1044171.pdf.

Varnes DJ (1978) Slope movement types and processes. In: Schuster RL, Krizek RJ (Eds.) Landslides, Analysis and Control, Transportation Research Board, Special Report No. 176, National Academy of Sciences, 11–33

von Ruette J, Lehmann P, Or D (2016) Linking rainfall-induced landslides with predictions of debris flow runout distances. Landslides 13(5):1097–1107. https://doi.org/10.1007/s10346-015-0621-2

Wang J, Jin W, Cui Y, Zhang W, Wu C, Alessandro P (2018) Earthquake-triggered landslides affecting a UNESCO Natural Site: the 2017 Jiuzhaigou Earthquake in the World National Park, China. J Mt Sci. https://doi.org/10.1007/s11629-018-4823-7

Wu YH (2021) Coupled empirical–mechanical modeling of debris flows occurred in small ungauged basins. Environ Earth Sci. https://doi.org/10.1007/s12665-020-09318-3

Wu CY, Chen SC (2013) Integrating spatial, temporal, and size probabilities for the annual landslide hazard maps in the Shihmen watershed. Taiwan Nat Hazards Earth Syst Sci 13(9):2353–2367. https://doi.org/10.5194/nhess-13-2353-2013

Xiao L, Wang J, Zhu Y, Zhang J (2020) Quantitative risk analysis of a rainfall-induced complex landslide in Wanzhou County, three Gorges reservoir, China. Int J Disaster Risk Sci 11:347–363. https://doi.org/10.1007/s13753-020-00257-y

Yergök AF, Akman Ü, İplikçi E, Karabalık N, Keskin N, Mengi H, Umut M, Armağan F, Erdoğan K, Kaymakçı H, Çetinkaya A (1987) The geology of West Black Sea. MTA General Directorate, 250 p, MTA Report No: 8273, Ankara

Zhang S, Zhang LM, Glade T (2014) Characteristics of earthquake- and rain-induced landslides near the epicenter of Wenchuan earthquake. Eng Geol 175:58–73. https://doi.org/10.1016/j.enggeo.2014.03.012

Zhang P, Ma J, Shu H, Han T, Zhang Y (2015) Simulating debris flow deposition using a two-dimensional finite model and Soil Conservation Service-curve number approach for Hanlin gully of southern Gansu (China). Environ Earth Sci 73:6417–6426. https://doi.org/10.1007/s12665-014-3865-6

Zhao B, Dai Q, Han D, Dai H, Mao J, Zhuo L, Rong G (2019) Estimation of soil moisture using modified antecedent precipitation index with application in landslide predictions. Landslides 16:2381–2393. https://doi.org/10.1007/s10346-019-01255-y

Zhu W, Liu K, Wang M, Nirandjan S, Koks EE (2022) Improved assessment of rainfall-induced railway infrastructure risk in China using empirical data. Nat Hazards. https://doi.org/10.1007/s11069-022-05605-3

Zhuang JQ, Iqbal J, Peng JB, Liu TM (2014) Probability prediction model for landslide occurrences in Xi'an, Shaanxi Province, China. J Mt Sci 11:345–359. https://doi.org/10.1007/s11629-013-2809-z

Zieher T, Gallotti G, Rianna G, Reder A, Pfeiffer J (2022) Exploring the effects of climate change on the water balance of a continuously moving deep-seated landslide. Nat Hazards. https://doi.org/10.1007/s11069-022-05558-7